Effects of confinement on the phase separation in emeraldine base polyaniline cast from 1-methyl-2-pyrrolidinone studied via dielectric spectroscopy

2002 J. Phys.: Condens. Matter 14 11769

(http://iopscience.iop.org/0953-8984/14/45/318)

INSTITUTE OF PHYSICS PUBLISHING JOURNAL OF PHYSICS: CONDENSED MATTER

J. Phys.: Condens. Matter **14** (2002) 11769–11778 PII: S0953-8984(02)52395-X

Effects of confinement on the phase separation in emeraldine base polyaniline cast from 1-methyl-2-pyrrolidinone studied via dielectric spectroscopy

Manuel R Bengoechea[1], **Fouad M Aliev**[1] **and Nicholas J Pinto**[2,3]

[1] Department of Physics, University of Puerto Rico, Río Piedras, PR 00931, USA
[2] Department of Physics and Electronics, University of Puerto Rico, Humacao, PR 00791, USA

E-mail: nj_pinto@cuhac.upr.clu.edu

Received 15 August 2002
Published 1 November 2002
Online at stacks.iop.org/JPhysCM/14/11769

Abstract

Measurement in the frequency range 3 mHz–10^6 Hz of the dielectric characteristics of emeraldine base polyaniline dissolved in 1-methyl-2-pyrrolidinone (NMP) and cast into bulk free-standing polymer films shows features similar to those reported by others and which are a result of microphase separation into reduced and oxidized repeat units. However, upon confinement into the cylindrical pores, of average diameter 20 nm, of a porous membrane such features of microphase separation do not occur. Strong pinning of the charge carriers due to interactions of the polymer with pore walls together with constrained chain packing and a non-uniform rate of evaporation of the NMP solvent from the pores suggests that the microphase separation observed in the bulk polymer is suppressed. This has the potential of being able to enhance the bulk conductivity after doping by reducing the internal intrachain disorder introduced by microphase separation.

1. Introduction

Conducting polymers have been a focus of attention among researchers for more than two decades, since the discovery of doped polyacetylene in the 1970s [1]. Their relatively large conductivity, light weight and flexibility are just some of the factors that make conducting polymers much more desirable than metals in certain applications. Of the various conducting polymers studied, polyaniline (PANi) has been investigated the most due to its ease of synthesis, relatively high conductivity and good stability. Depending on the oxidation level, PANi can be synthesized in various insulating forms such as the fully reduced leucoemeraldine base (LEB),

[3] Author to whom any correspondence should be addressed.

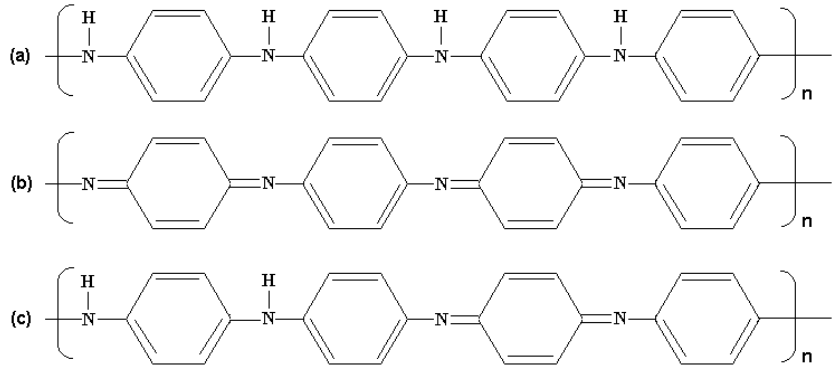

Figure 1. The three oxidation states of PANi: (a) fully reduced LEB, (b) fully oxidized PNB, (c) half oxidized/half reduced emeraldine base state (PANiEB).

half oxidized emeraldine base (PANiEB) and fully oxidized pernigraniline base (PNB) as seen in figure 1. Of these three forms, PANiEB is the most stable and widely investigated polymer in this family. PANiEB differs substantially from LEB and PNB in the sense that its conductivity can be tuned via doping from 10^{-10} up to 100 S cm^{-1} and more whereas the LEB and PNB forms cannot be made conducting. The insulating emeraldine base form of polyaniline (PANiEB) as seen in figure 1(c) consists of equal numbers of reduced and oxidized repeat units. The conducting emeraldine salt form (PANiES) is achieved by doping with aqueous protonic or functionalized acids where protons are added to the $-$N$=$ sites while maintaining the number of electrons in the polymer chain constant (non-redox doping). This leads to an increase in the conductivity by more than ten orders of magnitude [2] depending on the strength of the acid and method of processing [3–5]. The doping process can also be reversed by using ammonium hydroxide to reconvert the conducting salt form to the insulating base form.

PANiES is intractable and difficult to dissolve in common organic solvents, but PANiEB is soluble in 1-methyl-2-pyrrolidinone (NMP). Recently, it was reported that the observed dc conductivity of PANiES is a result of a small fraction ($<1\%$) of the available charge carriers contributing towards charge transport [6]. It has been suggested that the large number of isomeric forms that PANiEB can have leads to a less than optimum packing of polymer chains [7], thereby reducing interchain coherence. It was further shown via dielectric spectroscopy [8] and photoluminescence studies [9] that microphase separation of the oxidized and reduced repeat units took place in PANiEB dissolved and cast from NMP. Such microphase separation (the polymer chain consists of segments of LEB, PEB and PANiEB) [9] can affect the bulk conductivity of PANiEB films when cast from NMP and made conducting via acid doping since the phase separated regions cannot (in their pure form) be made conducting, thereby increasing the disorder that is responsible for lowering the bulk conductivity. Hence, studies aimed at suppressing such microphase separation during sample preparation need to be pursued.

In this investigation we have successfully impregnated PANiEB dissolved in NMP into the cylindrical pores of a porous membrane in order to study the effect of confinement on the microphase separation. We performed dielectric studies of the impregnated porous membrane mentioned above in the frequency range 3 mHz–10^6 Hz and found that upon drying the confined polymer does not show features of microphase separation as is the case in the bulk free-standing films cast from the same solution. The ability to dissolve the host membrane without affecting the encapsulated polymer yields itself to obtaining molecular size conducting wires when doped into the conducting state. This is the first low-frequency dielectric spectroscopy study

of PANiEB confined after polymerization into cylindrical porous membranes to address the above phenomenon of microphase separation. Previous studies [10, 11] on PANiES confined during synthesis had conductivities which were too high to permit low-frequency dielectric spectroscopy measurements.

2. Experimental section

2.1. Chemicals and sample preparation

Ammonium persulfate $(NH_4)_2S_2O_8$, hydrochloric acid HCl, ammonium hydroxide $(NH_4)OH$, 1-methyl-2-pyrrolidinone (NMP) C_5H_9NO and aniline $C_6H_5NH_2$ were purchased from Aldrich Chemicals and used without further purification. Using a method similar to that reported by Chiang and MacDiarmid [2], 2 ml of aniline was dissolved in 30 ml of 1 M HCl and kept at 0 °C, 1.15 g of $(NH_4)_2S_2O_8$ was dissolved in 20 ml of 1 M HCl also at 0 °C and added all at once under constant stirring to the aniline/HCl solution. The resulting dark green solution was maintained under constant stirring for 24 h, filtered and washed with water before being added to a 1 M $(NH_4)OH$ solution. After an additional 24 h the solution was filtered and a deep blue emeraldine base form of polyaniline was obtained (PANiEB). The filtrate was dried under dynamic vacuum for at least 24 h and used in the present work.

A 2 wt% solution of PANiEB and NMP was prepared by dissolving 103 mg of PANiEB in 5 ml of NMP and the solution was stirred for 48 h. The solution was then filtered through a 0.45 μm PTFE membrane and the resulting deep blue PANiEB/NMP solution appeared to be very uniform with no visible undissolved PANiEB. The PANiEB/NMP solution was placed in a glass bottle. A dielectrically inactive and rigid alumina Anopore cylindrical pore membrane was inserted into the bottle and capped. An Anopore membrane is a free-standing porous alumina disc of diameter 13 mm and thickness 60 μm with cylindrical parallel pores. The pores were of average diameter of 20 nm in this case and the axes of the cylindrical pores were perpendicular to the flat surface of the disc. Anopore membranes are commercially available and widely used in chromatography and dielectric spectroscopy in confined liquid crystals [12]. The solution of PANiEB/NMP with the porous membrane was kept in an oven at 80 °C for 24 h. The porous membrane was then taken out of the solution and had a uniform deep blue colour when held against the light. The porous membrane contained about 6 wt% of the polymer and the fill factor of polymer in the pores is roughly 50%. Free-standing PANiEB films were prepared from the same solution by casting onto glass slides kept in an oven at 80 °C. Once the NMP evaporated the films were then peeled off the slide by immersing the slide in water for a few seconds. Typical film thicknesses were of the order 15–20 μm. The bulk PANiEB/NMP free-standing film, henceforth labelled 'bulk polymer', and the polymer impregnated porous membrane, henceforth labelled 'confined polymer', were kept in a vacuum oven at 80 °C for 48 h and placed in a desiccator until the measurements were performed.

2.2. Experimental details

Measurements of the real (ε') and imaginary (ε'') parts of the complex dielectric permittivity (ε^*) in the frequency range 3 mHz–10^6 Hz were carried out using a Schlumberger Technologies 1260 impedance/gain-phase analyser in combination with a Novocontrol broad band dielectric converter and an active sample cell (BDC-S). The BDC-S with the active sample cell containing the sample holder, the sample capacitor, high-precision reference capacitors and active electronics optimizes the overall performance and reduces the typical noise in the measurements, particularly at low frequencies. The sample was mounted between two gold-plated parallel plates and placed in the closed cell at atmospheric pressure. The sample

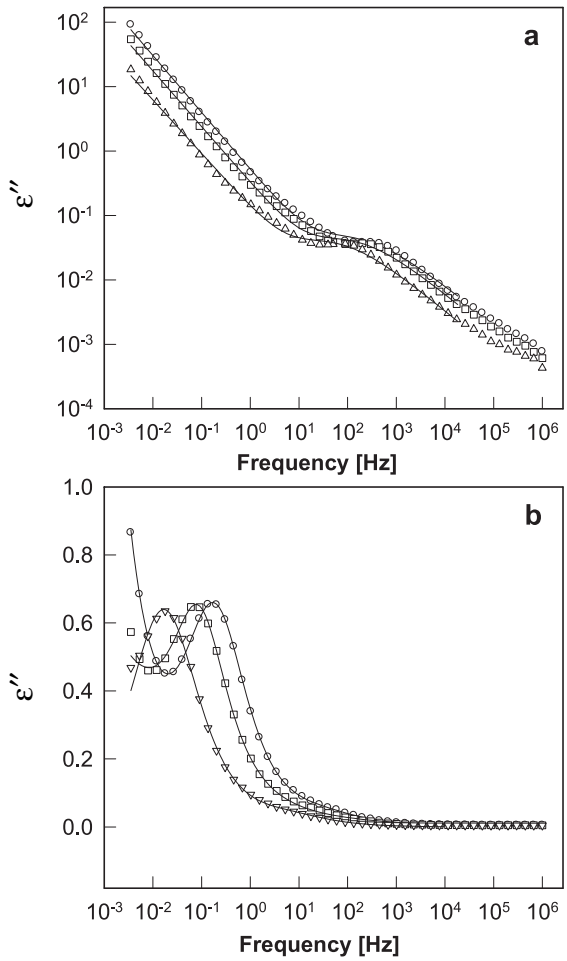

Figure 2. Frequency dependence of the imaginary part of the dielectric permittivity (ε'') for (a) the bulk polymer (log–log scale) and (b) the confined polymer (semilog scale) at different temperatures 343 (△), 363 (□) and 373 K (○). The solid curves are fits using the imaginary part of equation (1) in the text.

temperature was varied using filtered air flow through the sample cell and was controlled to within 0.1 °C using a Novocontrol temperature controller. Computer software (WinFit) provided with the dielectric spectrometer was used in the analysis of the data. The quantities measured directly by the spectrometer were the real and imaginary parts of the dielectric permittivity of the material under investigation as a whole. The porous membrane we used has negligible electrical conductivity, and its dielectric permittivities are practically independent of frequency and temperature. For this reason for the confined polymer we discuss below the temperature and frequency dependences of the measured dielectric permittivities and electric modulus of the composition membrane + polymer.

3. Results

Figures 2(a) and (b) show ε'' as a function of frequency on a log–log scale for the bulk polymer and on a semilog scale for the confined polymer respectively at three representative

temperatures of 343, 363 and 373 K. For the confined sample, the porous membrane (with the axes of the pores perpendicular to the membrane surface) was placed between two parallel metal plates which were connected to a dielectric spectrometer. Thus the probe electric field of the dielectric spectrometer was parallel to the cylindrical pore axis of the porous membrane. As seen in figures 2(a) and (b), ε'' shows noticeable differences in the confined polymer compared with the bulk polymer. While the confined polymer exhibits a clear peak, such a peak is obscured by the onset of dc conductivity in the bulk polymer in addition to being located at a higher frequency when compared with the confined polymer at the same temperature. Since the polymer under investigation is non-polar the observed peak in figures 2(a) and (b) is not associated with a structural relaxation and a dynamic glass transition (α-relaxation). We assign this relaxation process to the hopping and/or oscillations of charges around fixed pinning centres. These data in figure 2 were analysed using the Havriliak–Negami function shown below [13]:

$$\varepsilon^*(\omega) = -\mathrm{i}\frac{\sigma_o}{2\pi\varepsilon_o f^n} + \frac{\Delta\varepsilon}{(1+(\mathrm{i}2\pi f\tau)^\alpha)^\beta} + \varepsilon_\infty \tag{1}$$

where the first term on the right represents contributions from the dc conductivity, ε_o represents the permittivity of free space and ε_∞ represents the high-frequency limit of the real part of the dielectric permittivity, $\Delta\varepsilon$ represents the dielectric strength, τ is the relaxation time and f is the frequency of the probing electric field. The parameter α represents the width of the distribution while β describes the skewness of this distribution. Both parameters can take on values in the range from 0 to 1. The case $\alpha = 1$ and $\beta = 1$ represents the single-frequency Debye relaxation process. The relaxation processes in both samples studied here were of the non-Debye type with $\beta = 1$ and α ranging from 0.7 to 0.9 depending on the sample and temperature. These parameters correspond to the lower and higher temperatures studied respectively. The term $\mathrm{i}\sigma_o/2\pi\varepsilon_o f^n$ accounts for the contribution of ac conductivity. For Ohmic conductivity $n = 1$. The decrease of n, i.e. $n < 1$, could be observed, as a rule, if additionally to the contribution to ε'' from conductivity there is an influence of electrode polarization. Additionally n could be less than 1 in conducting polymers where the ac conductivity resembles that of phonon-assisted hopping [14]. As shown recently [14], multiple ac conduction mechanisms of the Austin and Mott type may also contribute to the measured ac conductivity leading to range of n values less than 1. Application of equation (1) for data analysis shows that the strong frequency dependence of ε'' for $f < 10$ Hz (bulk polymer) and $f < 0.1$ Hz (confined polymer) is due to both Ohmic conductivity and the contribution from electrode polarization. The solid lines shown in figures 2(a) and (b) indicate fits using equation (1). The values of n in the term describing the contribution of dc conductivity to ε'' varied from 0.9 to 0.8 for the bulk polymer in the temperature interval from 378 to 308 K respectively. Since $n < 1$, rigorously speaking we cannot relate σ_o to the dc conductivity, but for some temperature range $n = 0.9$, and if we assume that n is almost 1 then we can estimate σ_o and come to the conclusion that the bulk conductivity is greater that the conductivity of the confined sample. No significant contributions from the dc conductivity are seen in the confined polymer in the frequency range of interest, i.e. $f > 0.1$ Hz. The relaxation times calculated from this fitting process using the data in figures 2(a) and (b) are plotted in figure 3 according to the Arrhenius relation:

$$\tau = \tau_o \exp\left(\frac{E_a}{k_B T}\right), \tag{2}$$

where τ_o is the pre-exponential factor, E_a is the activation energy and k_B the Boltzmann constant. The relaxation times are seen to be shorter in the bulk polymer than in the confined polymer. It appears that the relaxation mechanisms are different for the bulk and the confined

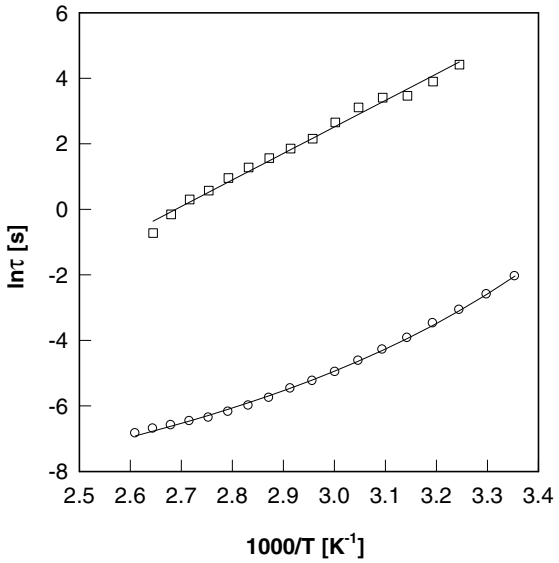

Figure 3. Relaxation times as calculated from fits to figures 2(a) and (b) using the imaginary part of equation (1) in the text plotted as a function of inverse temperature for the bulk (○) and confined polymer (□). The solid curves are fits to the data, using the Arrhenius relation (equation (2)) for the confined polymer and the Vogel–Fulcher relation (equation (3)) for the bulk polymer.

polymer. The relaxation time data for the bulk polymer were found to yield a better fit to the Vogel–Fulcher relation:

$$\tau = \tau_o \exp\left(\frac{B}{T - T_o}\right), \tag{3}$$

where T_o is the Vogel–Fulcher temperature that defines a temperature where relaxation time becomes infinitely large and B is a parameter characterizing the 'fragility' of the material [15]. In order to gain a qualitative insight into the relaxation processes seen in figures 2, the complex permittivity ε^* is converted to the complex electric modulus $M^*(= M' + \mathrm{i}M'') = 1/\varepsilon^* = E/D$, where E is the applied electric field and D is the dielectric displacement. Conductivity-related losses ε'' convert to a peak in M'' so conductivity-related processes are observed in both representations. Figures 4 and 5 show the real and imaginary parts respectively of M^* ($M' = \frac{\varepsilon'}{\varepsilon'^2+\varepsilon''^2}$; $M'' = \frac{\varepsilon''}{\varepsilon'^2+\varepsilon''^2}$) plotted as a function of frequency at representative temperatures of 343, 363 and 373 K for the bulk and confined polymers. Clear differences can be seen when figures 5(a) and (b) are compared with figures 2(a) and (b). For the bulk polymer as seen in figure 5(a), one well-resolved peak and a shoulder are seen, whereas for the confined polymer in figure 5(b) there is only one peak. Similar results were seen for bulk PANi polymer samples cast from NMP [8, 16] with the proposition that these peaks correspond to phase separated regions of the phase oxidized (peak at a lower frequency) and phase reduced (peak a at higher frequency) repeat units [8].

4. Discussion

4.1. Conductivity relaxation analysis

In conducting polymers there are no permanent dipoles. However, there is strong charge (polaron) trapping [17, 18], and its localized (short range) motion under the application of an

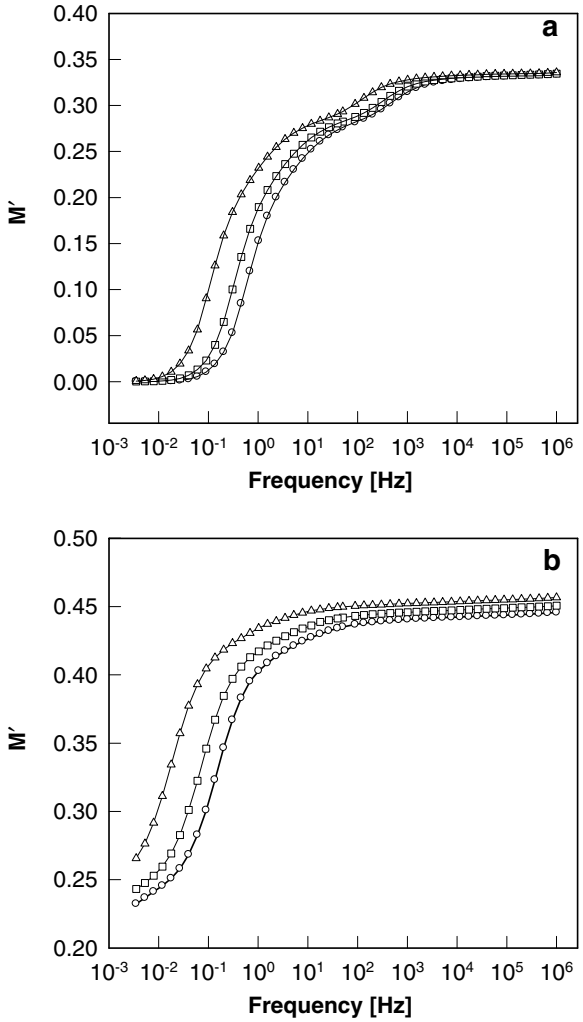

Figure 4. Frequency dependence of the real (M') part of the complex electric modulus (M^*) for the bulk polymer (a) and for the confiner polymer (b) at different temperatures: 343 (△), 363 (□) and 373 K (○). The solid curves are a guide to the eye.

external electric field serves as an 'effective' electric dipole. The dielectric relaxation in the presence of such an alternating electric field is a result of charge hopping among available localized sites [19]. For PANi in particular, which is a non-degenerate ground state polymer at low doping levels as is the case in this study, polarons and bipolarons formed during the doping and dedoping process are the relevant charge species [17, 20]. At low frequencies such charge hopping could extend throughout the sample in the absence of strong pinning leading to a continuous current. The relaxation process represented in figures 2 arises from hopping and/or oscillations of these charges around fixed pinning centres [17]. Increasing temperature has the effect of mobilizing the polymer chains, reducing pinning and thereby leading to a greater number of charges participating in the relaxation process for a fixed frequency. The value of the dc conductivity as extracted from the fits to the data in figures 2(a) and (b) at 373 K is 2.66×10^{-13} S cm^{-1} for the bulk polymer and 1.1×10^{-16} S cm^{-1} for the material

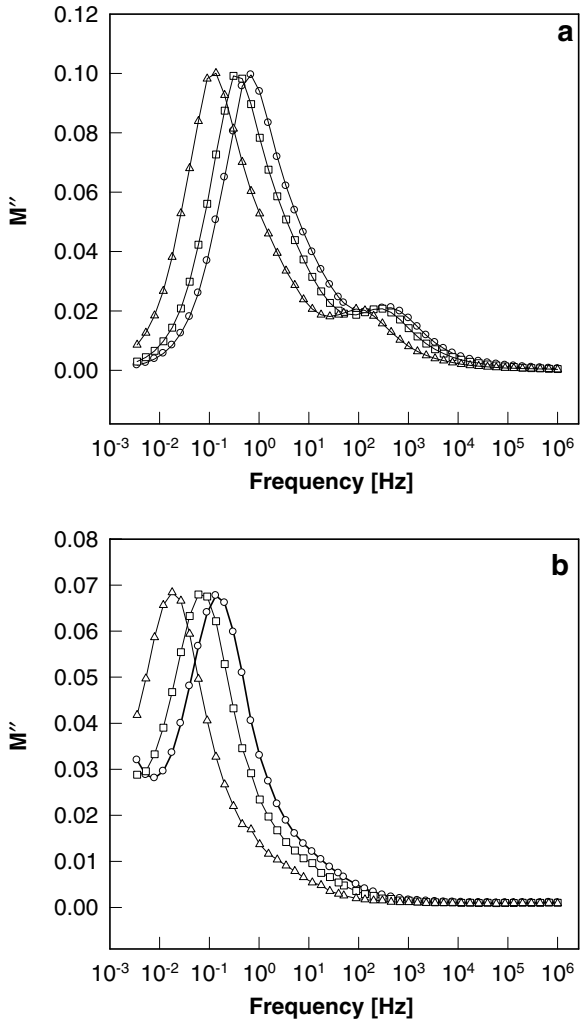

Figure 5. Frequency dependence of the imaginary part (M'') part of the complex electric modulus (M^*) for the bulk polymer (a) and for the confiner polymer (b) at different temperatures: 343 (△), 363 (□) and 373 K (○). The solid curves are a guide to the eye.

containing the confined polymer. Taking into account that the weight fraction of the confined polymer is about 6% of the weight of the whole sample we can estimate the conductivity of the confined polymer itself as 1.8×10^{-15} S cm^{-1}. The conductivity of the bulk polymer was temperature dependent, varying from 8.9×10^{-13} to 1.9×10^{-15} S cm^{-1} in the temperature range 383–298 K. For the confined polymer there was very weak temperature dependence of conductivity at relatively high temperatures $T > 330$ K. At temperatures below 330 K there was almost no contribution of the conductivity to the measured dielectric spectra. The substantial decrease of the dc conductivity for the confined polymer as seen in figure 2(b) is an indication that interactions of the polymer with the pores have substantially pinned the charge carriers preventing charge transport, which is not the case for the bulk polymer. In both samples, increasing the temperature shifts the peak towards higher frequencies as a result of shorter time constants associated with increased chain movement. However it must be stated that increased

chain movement does not imply efficient charge transport as there is a concomitant reduction in polymer conjugation at higher temperatures thereby increasing barrier potentials for charge transport. This effect is seen in figure 3 where the relaxation times for both polymers (bulk and confined) are plotted as a function of reciprocal temperature. The parameters as calculated from equation (2) for the confined sample were $\tau_o = 3.57 \times 10^{-10}$ s, $E_a = 0.69$ eV while for the bulk sample, it was found that the Vogel–Fulcher relation of equation (3) gave a better fit with $\tau_o = 1.12 \times 10^{-5}$ s, $B = 730$ K and $T_o = 220$ K. Such a change in the mechanism could be attributed to the different chemical environments encountered by the relaxing charges due to microphase separation of the polymer into LEB, PNB and PANiEB phases in one sample and not the other, as discussed later. Charge absorption in two-component heterogeneous media gives rise to dispersion of dielectric permittivity which develops according to the following scenario: for a mixture of two or more components the accumulation of charges at the interfaces between phases give rise to a polarization which contributes to the relaxation if at least one component has non-zero electric conductivity. This phenomenon is known as the Maxwell–Wagner (MW) effect [21]. The MW process is described by the Debye relaxation function. In our case, for the confined polymer, the relaxation process is not described by the Debye relaxation function as it should be for the MW relaxation and there is a spectrum of relaxation times. Therefore it is difficult to attribute the observed low-frequency relaxation process for a confined polymer to the MW relaxation. We believe that this relaxation process is related to charge hopping as mentioned earlier, as observed in the bulk but modified by confinement.

For the confined sample having constrained chain packing the additional barriers introduced by polymer interactions with the pore walls lead to charge trapping thereby reducing the probability of charge transport as evidenced by a decrease in the dc conductivity. This would explain the longer relaxation times when compared with the bulk. The presence of NMP between polymer chains is also likely to affect relaxation dynamics due to greater chain separation [8]. Such an effect will be more prominent in the confined polymer as pore filling occurs due to the flow of NMP into the pores and which when evaporated would lead to larger chain separation than in the bulk.

4.2. Electric modulus analysis

PANiEB when dissolved and cast from NMP shows microphase separation into fully oxidized and fully reduced regions [8]. Such phase separation could occur as a result of the rapidly changing diblock nature of the polymer in solution which must freeze upon slow controlled evaporation of the solvent [9]. The presence of a strong peak and a weak shoulder in the imaginary part of the electric modulus (M'') for the bulk polymer film as seen in figure 5(a) is similar to that reported earlier [8, 16] and is a result of microphase separation of the polymer chain into segments of LEB, PNB and PANiEB. This double peak attribute of M'' is not seen in the confined polymer (figure 5(b)) implying that there is no microphase separation. Figures 4(a) and (b) also show slight differences between the bulk and confined polymers, although the differences are much more pronounced in figures 5(a) and (b). Data taken on a pressed pellet of the bulk PANiEB powder (free of NMP) also show one peak and hence no phase separation. The NMP solvent which acts as a plasticizer has a high boiling point (202 °C) and is thus difficult to remove completely upon drying. Thus any finite amount of NMP in the polymer will assist in phase separation and present structural barriers to increasing the bulk conductivity in addition to increasing interchain separation. Dielectric permittivity results as discussed in the previous section show that in the confined polymer there is strong pinning of the charge carriers due to interaction of the polymer with the parallel pore walls, and this together with constrained longitudinal chain packing and a non-uniform rate of evaporation of the NMP solvent from the pores

suggests that microphase separation as observed in the bulk polymer is suppressed. For the bulk polymer the shoulder at higher frequency is much weaker than the low-frequency peak for all measured temperatures, indicating a greater concentration of the phase oxidized repeat units.

5. Conclusion

Dielectric characteristics of bulk films of PANiEB dissolved and cast from NMP are similar to the bulk data published earlier by others, suggesting microphase separation of the oxidized and reduced repeat units in PANiEB. However, when confined into parallel cylindrical pores of average diameter 20 nm, this phase separation is seen to be suppressed due to charge pinning arising from interactions of the polymer with the pore walls, constrained longitudinal chain packing and the non-uniform rate of evaporation of the solvent from the pores.

Since the confined polymer does not show characteristics of microphase separation and hence reduced intrachain disorder, doping should result in higher conductivity than in the bulk counterpart. Efforts are under way to dissolve the porous membrane after sample annealing to remove most of the NMP and extract nanofibres of the polymer. Results of characterization of these nanofibres will be presented in the future.

Acknowledgments

The authors would like to thank Dr Sergey Filippov for initial work done on this project. This work was supported by the Office of Naval Research under grant number N00014-99-1-0558 and NSF grant DMR-0098603.

References

[1] Chiang C K, Fincher C R Jr, Park Y W, Heeger A J, Shirakawa H, Louis E J, Gau S C and MacDiarmid A G 1977 *Phys. Rev. Lett.* **39** 1098–101
[2] Chiang J C and MacDiarmid A G 1986 *Synth. Met.* **13** 193–205
[3] Monkman A P and Adams P 1991 *Synth. Met.* **40** 87–96
[4] Cao Y, Smith P and Heeger A J 1992 *Synth. Met.* **48** 91
[5] Wang Y Z, Joo J, Hsu C-H, Pouget J P and Epstein A J 1994 *Macromolecules* **27** 5871–6
[6] Kohlman R S, Zibold A, Tanner D B, Ihas G G, Ishiguro T, Min Y G, MacDiarmid A G and Epstein A J 1997 *Phys. Rev. Lett.* **78** 3915–18
[7] MacDiarmid A G, Zhou Y and Feng J 1999 *Synth. Met.* **100** 131–40
[8] Lee H T, Chuang K R, Chen S A, Wei P K, Hsu J H and Fann W 1995 *Macromolecules* **28** 7645–52
[9] Shimano J Y and MacDiarmid A G 2001 *Synth. Met.* **123** 251–62
Shimano J Y and MacDiarmid A G 2001 *Synth. Met.* **119** 365–6
[10] Wu C G and Bien T 1994 *Science* **264** 1757–9
[11] Zarbin A J G, DePaoli M A and Alves O L 1999 *Synth. Met.* **99** 227–35
[12] Batalla B, Sinha G P and Aliev F M 1999 *Mol. Cryst. Liq. Cryst.* **331** 1981–5
[13] Havriliak S and Negami S 1966 *J. Polym. Sci. Part C* **14** 99
[14] Papathanassiou A N 2002 *J. Phys. D: Appl. Phys.* **35** L88–9
[15] Richert R and Blumen A (ed) 1994 *Disorder Effects on Relaxational Processes* (Berlin: Springer)
[16] Calleja R D, Matveeva E S and Parkhutik V P 1995 *J. Non-Cryst. Solids* **180** 260–5
[17] Javadi H H S, Zuo F, Cromack K R, Angelopoulos M, MacDiarmid A G and Epstein A J 1989 *Synth. Met.* **29** E409–16
Zuo F, Angelopolous M, MacDiarmid A G and Epstein A J 1989 *Phys. Rev.* B **39** 3570–8
[18] Papathanassiou A N, Grammatikakis J, Sakkopoulos S, Vitoratos E and Dalas E 2002 *J. Phys. Chem. Solids* **63** 1771–8
[19] Jonscher A K 1983 *Dielectric Relaxation in Solids* (London: Chelsea)
Jonscher A K 1999 *J. Phys. D: Appl. Phys.* **32** R57–70
[20] Pinto N J, Acosta A A, Sinha G P and Aliev F M 2000 *Synth. Met.* **113** 77–81
[21] Scaife B K P 1989 *Principles of Dielectrics* (Oxford: Clarendon)